

**The 200,000 m<sup>3</sup>/day Hamma Seawater Desalination Plant –  
Largest Single-Train SWRO Capacity in the World and Alternative to Pressure Center Design**

**Authors:**

Richard L. Stover, Ph.D.; Energy Recovery, Inc.; Tel: +1-510-483-7370, stover@energy-recovery.com  
Jeremy Martin; Energy Recovery, Inc.; Tel: +1-510-483-7370, jmartin@energy-recovery.com  
Michael Nelson, Ph.D. P.E.; GE Ionics; Tel: +1-408-865-0830, mbnelson@pacbell.net

**Presenter:**

Richard L. Stover, Ph.D.

**Abstract**

The GE Infrastructure (Ionics) Hamma Algeria project is a seawater reverse osmosis (SWRO) desalination plant capable of continuously producing 200,000 cubic meters of permeate per day. The Hamma plant is intended to supply 25% of Algeria's capital city's population with desperately needed drinking water. The project is the first private reverse osmosis potable water project in Algeria and the largest membrane desalination plant in Africa. The plant comprises nine trains, each capable of continuously producing 25,100 cubic meters per day of permeate, making them the highest-capacity SWRO trains in the world. Each SWRO train is equipped with a dedicated high-pressure pump, booster pump and array of PX Pressure Exchanger energy recovery devices.

The design of the plant included hydraulic modeling of the flow distribution in the 32-unit arrays of PX devices. The flow analysis, which produced some counter-intuitive results, has significant implications for the design of manifold systems in general, including membrane arrays, energy recovery device arrays and multiple pumps operating in parallel. The authors discuss the considerations in pumping system, train size and energy recovery system configuration in large-train SWRO plants to maximize operational efficiency, flexibility and uptime.

## I. INTRODUCTION

As the scale of seawater reverse osmosis (SWRO) desalination plants has increased, engineers have sought higher capacity components. In addition to supplying more flow, higher capacity pumps are generally more efficient. However, neither membranes elements nor isobaric (positive displacement) energy recovery devices (ERDs) are more efficient in larger sizes, and the mechanical complexity and maintenance requirements of larger elements can be prohibitive. Fortunately, arrays of membrane elements and ERDs typically operate with the same efficiency as individual devices. Accordingly, the design and deployment of multiple units in arrays has become standard practice (1).

Flow distribution in an array of devices or components is an issue of concern in many hydraulic applications. In SWRO, proper manifold design for even flow distribution is important for energy recovery device arrays, membrane arrays or when multiple trains or pumps are connected to common headers. This paper describes the pumping system, train size and energy recovery system configuration of the GE Infrastructure (Ionics) project in Hamma, Algeria (Hamma).

## II. HAMMA ALGERIA SWRO PLANT

The Hamma project is an SWRO plant capable of continuously producing 200,000 cubic meters of permeate per day ( $m^3/d$ ). The Hamma plant is intended to supply 25% of Algeria's capital city's population with desperately needed drinking water. The project is the first private reverse osmosis potable water project in Algeria and the largest membrane desalination plant in Africa.

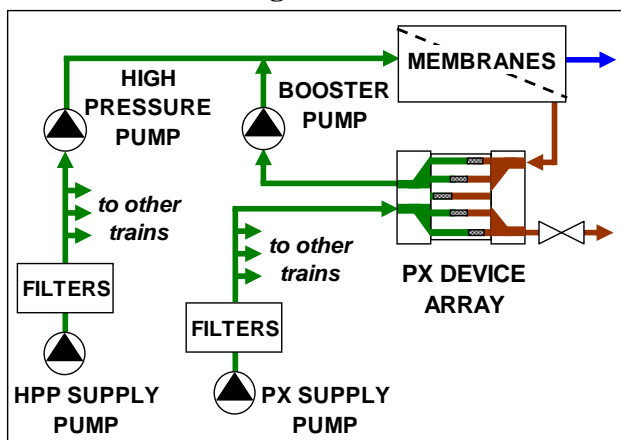
The plant is fed with open intake Mediterranean seawater with a salinity of 38 to 40 grams per liter (g/L) and a temperature of 15 to 27 degrees Celsius (degC). It is designed to work at a membrane recovery rate of 40.0 to 44.5 percent. Brine is discharged from the pressure exchanger units at a pressure of 0.7 bar for transfer back to the Mediterranean sea through a pipe outfall.

A schematic diagram of the main components of the reverse osmosis process is shown in Figure 1 below. The plant comprises nine first-pass trains, each capable of continuously producing 25,100  $m^3/d$  of permeate, making them the highest-capacity SWRO trains in the world. The membrane elements of each train are fed with a dedicated high-pressure pump (HP pump), booster pump and array of thirty-two (32) ERI<sup>®</sup> model PX-220 PX Pressure Exchanger<sup>®</sup> energy recovery devices. All nine HP pumps are fed from a common supply manifold. This manifold is maintained at a pressure greater than 3.5 bar to meet the minimum net positive suction pressure requirement of the HP pumps. The supply flow rate and pressure can be adjusted with a variable frequency driver on the HP pump supply pump which in turn varies the flow rate and output pressure of the HP pumps.

---

® ERI, PX, PX Pressure Exchanger and the ERI logo are registered trademarks of Energy Recovery, Inc.

**Figure 1 – Schematic Diagram of Hamma SWRO Process**



The PX device arrays are fed from a second supply manifold that is maintained at a pressure of greater than 1.3 bar to meet the minimum discharge-pressure-requirement of the PX devices. Because the PX device arrays and HP pumps are supplied separately, the PX device arrays are isolated from flow and pressure variations that can occur as individual HP pumps go on- and off-line. This supply configuration also minimizes the overall supply pressure required by the plant because the inlet pressure requirement of the PX arrays is significantly lower than that of the HP pumps.

The Hamma plant was designed for both high capacity and minimum operating cost. Because pumps consume most of the energy supplied to the plant, it was essential that they be designed for high operating efficiency. As described by the Hydraulic Institute, larger centrifugal pumps are generally more efficient than smaller pumps, and the peak efficiency for very large centrifugal pumps is about 89% (2). The HP pumps selected for the Hamma plant operate at 1,084 m<sup>3</sup>/hr and approximately 88% efficiency, close to the theoretical maximum for the centrifugal pumps and notably high for high-head service. The booster pumps are also large, operating at 1,351 m<sup>3</sup>/hr and 89% pump efficiency.

An alternative to large trains is to feed multiple smaller trains with the same HP pump in a process configuration known as a pressure center design. One of the advantages of this design is that larger, more efficient HP pumps can be used than if the individual trains were supplied separately. The SWRO plants in Ashkelon, Israel and in Kwinana (Perth), Australia utilize pressure center designs (3)(4). However, because the Hamma trains are so large, the HP pumps operate at nearly the same efficiency as those in the large pressure-center plants. Although pressure-center plants can, in theory, operate with a number of pumps or SWRO trains offline for maintenance, the process controls and valves necessary for full flexibility can add expense and operational complexity. An advantage of Hamma's dedicated high pressure pumps is that each train can be operated independently, thereby facilitating relatively easy startup, shutdown and optimization of membrane recovery rate.

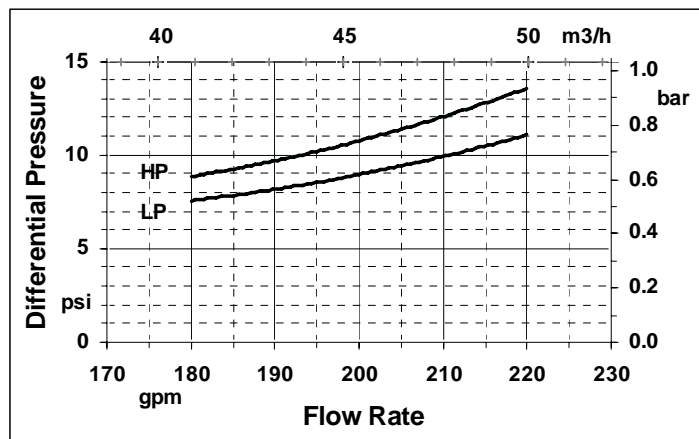
### **III. PX PRESSURE EXCHANGER ENERGY RECOVERY DEVICES**

In a SWRO system equipped with PX Pressure Exchanger energy recovery devices, the membrane reject is directed to the membrane feed (through the PX devices and booster pump) as illustrated in Figure 1 above. A rotor, moving between the high-pressure and low low-pressure stream, removes the brine and replaces it with seawater. Pressure transfers directly from the high-pressure reject stream to a feed stream with no intervening piston in the flow path. The direct contact between the brine and seawater results in an increase in salinity at the membrane feed of 1 to 2.5% compared to raw seawater. The

mixing in the rotor is minimized with long, small diameter chambers and a short brine-seawater contact time (0.05 seconds). The rotor spins freely, driven by the flow at a rotation rate proportional to the flow rate, so feed flow rates must be limited to avoid excess rotor speed. However, unlimited capacity can be achieved by arraying multiple devices in parallel. A total energy transfer efficiency of up to 98% is possible, and efficiency is nearly constant over a wide range of flow and pressure variations.

The flow-pressure performance of a PX-220 Pressure Exchanger device is illustrated in Figure 2. Head loss in a PX unit is primarily the result of frictional losses as the water flows through the rotor. Since each PX rotor is a precision device machined to extremely tight tolerances, there is very little performance variation unit to unit. Each PX stays on its characteristic curve and is controlled by the flow rather than with valves, sensors, or computers which often malfunction in marine environments.

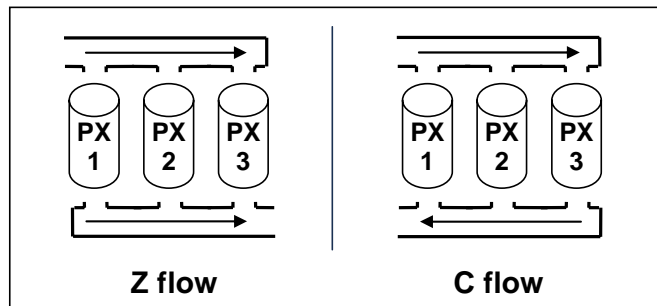
**Figure 2 – PX-220 Device Characteristic Curves**



#### IV FLOW IN MANIFOLDS

Manifolds can be configured in a number of ways with respect to the inlet and outlet of the bulk flow. Two possible configurations for arrays of PX units are illustrated in Figure 3 below. If the flow enters and exits the manifolds at opposite ends of the array, the flow scheme is termed “Z-flow” which roughly describes the pattern of the flow through the array. An array in which flow enters and exits at the same end will be called a “C-flow” scheme in this analysis.

**Figure 3 – Manifold Flow Schemes**



For arrays of passive-flow elements, such as PX devices or SWRO membrane vessels, the flow across a given lateral is driven by the differential pressure across the element. For PX devices, differential pressure drives flow according to Figure 2. The pressure at any point along a manifold depends upon the

velocity, friction and elevation. This relationship is described by the Navier-Stokes equations, which are formulations of mass, momentum and energy conservation laws for Newtonian fluid flows (5). These equations are supplemented with state equations defining the viscosity and density of the fluid. Although fluid properties can vary with the pressure, salinity and temperature changes encountered in SWRO systems, the density changes in a given manifold are generally small enough so that an assumption of incompressibility is valid.

For steady state flow of incompressible fluids, the Navier-Stokes equations reduce to the following equation useful for turbulent flow calculations in piping systems:

$$\frac{P_2 - P_1}{\rho} + \frac{v_2^2 - v_1^2}{2} + g \times (Z_2 - Z_1) + \sum f = 0 \quad (1)$$

where:

P = pressure,

$\rho$  = density,

v = velocity,

g = gravitational constant,

Z = elevation,

$\sum f$  = sum of piping and fitting resistances, and

the numerical indexes refer to two arbitrary locations in the system.

In the limit of a very large manifold header, the velocity terms in Equation (1) become small, the manifold begins to resemble a constant-pressure reservoir, and the variation of flow through the laterals becomes negligible. However, very large manifold headers are generally not practical because of material and construction costs.

Considering Equation (1) in the context of the manifold flow schemes illustrated in Figure 3 above, elevation changes in a given header can be ignored. The local velocity in the inlet (upper) header in each configuration decreases as water diverts into the PX units causing a pressure increase in the direction of flow. Friction in the header and across the fittings tends to decrease pressure in the direction of flow. Therefore, the velocity change and friction have opposing affects on the local pressure in the inlet header. In the outlet header, velocity increases in the direction of flow which tends to decrease the local pressure. Friction also decreases pressure in the direction of flow.

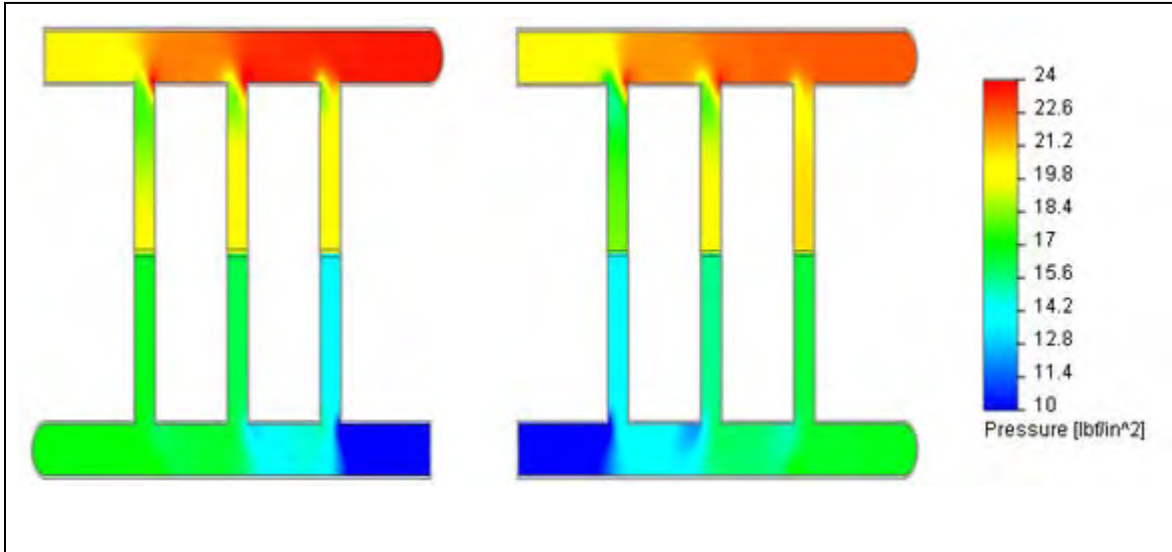
## V. COMPUTATIONAL FLUID DYNAMICS ANALYSIS

For quantitative analysis of flow through a manifold, the Navier-Stokes equations were solved using COSMOSFloWorks 2006 computational fluid dynamics (CFD) software. COSMOSFloWorks employs a finite volume method on a spatially-rectangular computational mesh refined locally at the solid/fluid interfaces and in the fluid region during calculation. The equations were discretized over the mesh elements, spatial derivatives were approximated with implicit-difference operators of second-order accuracy, and time derivatives were approximated with an implicit first-order Euler scheme.

The software was run for a simplified manifold design, similar to that illustrated in Figure 3 above, but using porous wafers instead of PX devices to constrict flow through the laterals. The CFD results for the pressure distribution in Z- and C-flow manifold schemes are shown in Figure 4 below. In the Z-flow

scheme, the pressure in the inlet header is highest at the blind end where the velocity is lowest. The corresponding result is that friction has much less influence on the pressure distribution than the velocity change. For the inlet header, this means that pressure increases in the direction of flow. This result is counter-intuitive to many.

**Figure 4 – Computational Fluid Dynamics Results – Pressure Distribution in a Simplified Array**



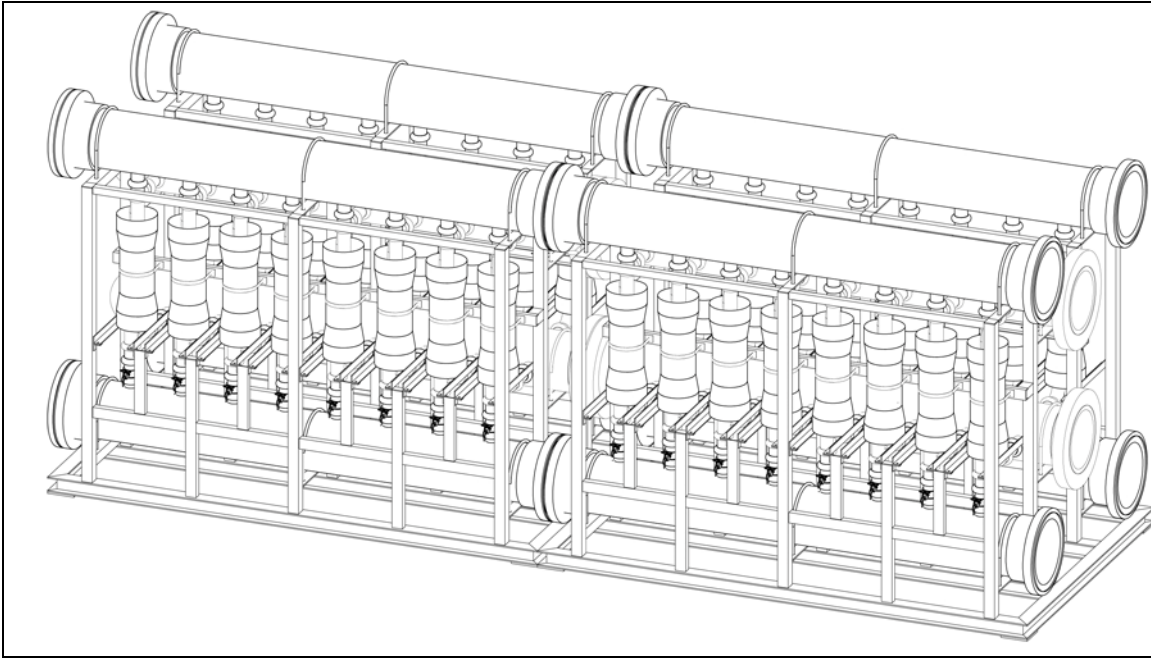
In the C-flow configuration, pressure is also highest at the blind ends of the inlet and outlet headers. Because the pressure gradient in the inlet header is similar to the pressure gradient in the outlet header, the pressure difference across each element is approximately equal. Therefore the flow through each element in the C-flow manifold can be expected to be more constant than in a Z-flow manifold.

Flow variation in an array fed by very large diameter headers is uniform regardless of flow configuration. Although a small-diameter header would increase the influence of friction, the velocity would also increase and the influence of the velocity change on pressure would be expected to increase accordingly. This trend was verified with CFD analysis results not shown here. In all headers, pressure is highest near the blind end of the manifold where the velocity of the flow is the lowest. In general, C-flow manifolds provide a more constant pressure difference across each element resulting in a more even flow distribution in an array than provided by Z-flow manifolds.

**IV. PX DEVICE ARRAYS AT HAMMA**

A schematic representation of the Hamma project’s 32-element PX device arrays is given in Figure 5 below. High-pressure water flows through two 16-inch nominal-diameter schedule-40 stainless-steel headers located in the center of the array. The thirty-two branches are arranged in pairs oriented 180 degrees around the header at each of the 16 axial positions. Low-pressure water to the array flows through four 16-inch schedule 80 PVC headers located directly above and below the PX devices. The lateral branches are 3-inch nominal diameter schedule 80 on all headers, spaced 356 millimeters on center. The design flow rate through the PX arrays for both high- and low-pressure is 1,380 m<sup>3</sup>/hr/SWRO train. Therefore, the design flow rate at the high-pressure inlet is 1,380 m<sup>3</sup>/hr and the flow rates at both low-pressure outlets are 690 m<sup>3</sup>/hr. The fluid properties used for the simulations were those of seawater at 25 degC and 38 g/L total dissolved solids.

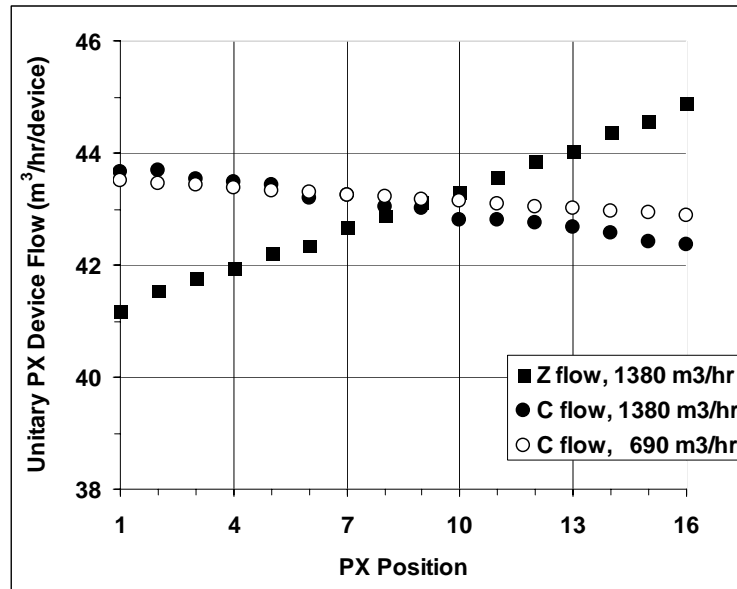
**Figure 5 – Hamma PX Device Array**



The pressure and flow distributions in the Hamma PX device manifolds were simulated for both Z- and C-flow configurations. To save computational time, an iterative method was employed and the inlet and outlet manifolds were analyzed separately. In the first pass, the flow rate at each branch was initially set to the average unitary flow rate. The software was run and the pressure at each branch was recorded. The differential pressure across each lateral and Figure 2 were used to calculate the flow rate through each PX device in the array. The differences between the calculated flow rates and the initially-assumed flow rates were noted as errors. The calculated flow rates were assumed for the second iteration and the program was run again. The new pressure distribution was again used to calculate the flow distribution according to Figure 2. Iteration in this manner continued until the errors reduced to less than 0.2%. This typically took two or three iterations.

The results of the flow simulations are presented in Figure 6 below. Flow through the PX devices in a Z-configuration ranged from 4.3% below the average at the position closest to the entrance of the inlet manifold to 4.3% above the average at the position closest to the blind end of the inlet manifold. The same bulk flow rate through a PX array arranged in a C-flow configuration resulted in a unitary flow of 1.5% above the average at the inlet ends to 1.6% below the average at the blind ends. Reducing the bulk flow rate in the C-flow configuration by a factor of two decreased the range of flows to + or - 0.7% of the average.

**Figure 6 – Summary of Computational Fluid Dynamics Modeling Results**



GE Ionics chose a C-flow scheme for the PX device arrays at Hamma because of the more even flow distribution provided by that configuration.

## VII. CONCLUSION

The Hamma, Algeria SWRO plant utilizes large trains with dedicated high-pressure pumps, booster pumps and PX Pressure Exchanger energy recovery device arrays to achieve maximum energy efficiency. Pump performance at Hamma is comparable to what could be achieved with a pressure center design but with greater ease of operation.

The analysis of flow distribution along an array of PX devices presented herein showed that the change in velocity along a manifold has a greater influence on the pressure distribution and corresponding flow distribution than friction does in most manifolds. This analysis supports the general conclusion that a C-flow-manifold configuration with properly-sized headers provides more even flow distribution along an array than a Z-flow-manifold configuration.

## VIII. REFERENCES

- (1) R.L. Stover, Seawater Reverse Osmosis with Isobaric Energy Recovery Devices, *Desalination* 203 (2007) 168-175.
- (2) The Hydraulic Institute, [www.pumps.org](http://www.pumps.org).
- (3) B. Lieberman and M. Faigon, Flexible 3-Centre Setup Saves Costs in Ashkelon, *Desalination & Water Reuse*, 1414 (2005) 19-21.
- (4) M.A. Sanz and R.L. Stover, Low Energy Consumption in the Perth Seawater Desalination Plant, *Proceedings of the International Desalination Association World Congress, Maspalomas, Gran Canaria* (2007).
- (5) R.B. Bird, W.E. Stewart and E.N. Lightfoot, *Transport Phenomena*, John Wiley and Sons (1960) 203-216.